

Critical behavior of the ferromagnetic perovskites RTiO_3 ($R = \text{Dy, Ho, Er, Tm, Yb}$) by magnetocaloric measurements

Yantao Su,¹ Yu Sui,^{1,*} J.-G. Cheng,^{2,3} J.-S. Zhou,² Xianjie Wang,¹ Yang Wang,¹ and J. B. Goodenough²

¹*Department of Physics, Harbin Institute of Technology, Harbin 150001, China*

²*Texas Materials Institute, University of Texas at Austin, Austin, Texas 78712, USA*

³*Institute of Physics, Chinese Academy of Sciences, Beijing 100190, China*

(Received 6 November 2012; published 2 May 2013)

Ferromagnetism in perovskites RTiO_3 can be induced by a steric effect. The way in which the subtle local structural change can induce three-dimensional (3D) ferromagnetic coupling through Ti-O-Ti superexchange interactions remains controversial. A critical behavior study for the ferromagnetic phase has been made so far only on YTiO_3 because the magnetization measurements are plagued by the contribution from the magnetic rare earth. Here we report critical exponents for most ferromagnetic members in the RTiO_3 family by measuring the magnetocaloric effect and applying the corresponding scaling laws. Our results indicate that the ferromagnetic coupling in the RTiO_3 can be well described by the 3D Heisenberg model.

DOI: [10.1103/PhysRevB.87.195102](https://doi.org/10.1103/PhysRevB.87.195102)

PACS number(s): 75.40.Cx, 75.30.Sg, 75.47.Lx

For a second-order ferromagnetic phase transition, the critical behavior near the Curie temperature T_c is characterized by a set of critical exponents¹ α , β , γ , and δ , associated with, respectively, the specific heat C , the spontaneous magnetization M_s ($\equiv M_{H=0}$), the initial magnetic susceptibility χ_0 ($\equiv \partial M / \partial H|_{H=0}$), and the critical isothermal $M(H)_{T=T_c}$ through the following equations:

$$C(T) \sim |T - T_c|^{-\alpha}, \quad (1)$$

$$M_s(T) \sim |T - T_c|^\beta \quad (T < T_c), \quad (2)$$

$$\chi_0(T) \sim |T - T_c|^{-\gamma} \quad (T > T_c), \quad (3)$$

$$M(H) \sim H^{1/\delta} \quad (T = T_c). \quad (4)$$

These critical exponents are not independent, and the number of independent variables is reduced to two by the following relations:

$$\alpha + 2\beta + \gamma = 2, \quad (5)$$

$$\delta = 1 + \gamma/\beta. \quad (6)$$

Precise determination of these critical exponents can provide valuable information about a magnetic phase transition, e.g., the range and the dimensionality of the magnetic exchange interactions.² As shown in Table I, distinct values of the critical exponents corresponding to different models have been derived theoretically.¹ The mean-field model with $\alpha = 0$, $\beta = 0.5$, and $\gamma = 1$ signals a long-range exchange interaction with negligible critical fluctuations near T_c . Such critical behaviors are usually observed in the very weak itinerant-electron ferromagnetic systems, e.g., ZrZn_2 ,³ which have been justified theoretically by Stoner and Wohlfarth.⁴ In contrast, the three-dimensional (3D) Heisenberg model involves isotropic nearest-neighbor exchange interactions between localized spins; significant critical fluctuations in the vicinity of T_c lead to $\beta < 0.5$ and $\gamma > 1$. Such a universality class has been found experimentally in a wide range of ferromagnetic systems, including metallic Ni,⁵ CrO_2 ,⁶ $\text{La}_{1-x}\text{A}_x\text{MnO}_3$,⁷ and insulating YTiO_3 .^{8,9} Although the 3D Ising model is applicable when the spin degree of freedom is restricted to one direction,

an experimental realization of the 3D Ising ferromagnetism in real systems is rare.¹⁰

For a critical behavior analysis around a second-order ferromagnetic transition, the most straightforward and widely used approach is the Arrott-plot method,¹¹ based on direct current (dc) magnetization measurements. For this purpose, a series of isothermal magnetization $M(H)$ curves around T_c is replotted in the form of M^2 versus H/M , i.e., the Arrott plot. A parallel linear Arrott plot signals the mean-field universality class with $\beta = 0.5$ and $\gamma = 1$. However, in most cases, the Arrott plot does not produce straight lines. In order to determine precisely the critical exponents, these isotherms in the Arrott plot are usually fitted with a polynomial function and then extrapolated to the $H/M = 0$ and $M^2 = 0$ axes to obtain the spontaneous magnetization M_s and the initial magnetic susceptibility χ_0 , respectively. Then, a power law fitting to $M_s(T)$ and $\chi_0(T)$ according to Eqs. (2) and (3) yields the values of β and γ , respectively. By using these critical exponents as a starting point, a modified Arrott plot, $M^{1/\beta}$ versus $(H/M)^{1/\gamma}$, can be obtained, and the above procedures can be applied again to get new values of β and γ . Such an iteration process can be applied until the critical exponents β and γ converge. Parallel straight isothermal lines should be restored in the modified Arrott plot with the correct critical exponents.

For most homogeneous ferromagnetic systems involving only one magnetization process, the above-mentioned Arrott-plot method is applicable. Otherwise, application of this method requires caution; interpretation of the obtained critical exponents must take into account the specific situation of the magnetic system. For example, in the RTiO_3 ($R = \text{Gd}, \dots, \text{Lu}, \text{ and Y}$) perovskites, the critical behavior associated with the ferromagnetic ordering of the localized $\text{Ti}^{3+} S = \frac{1}{2}$ spin can be well understood in terms of the 3D Heisenberg model as shown in YTiO_3 . However, in these ferromagnetic RTiO_3 ($R \neq \text{Y and Lu}$), the presence of large paramagnetic R^{3+} moments near T_c makes the Arrott-plot method invalid for the critical-behavior analysis. As shown in the present study on RTiO_3 , the Arrott-plot approach even leads to an opposite conclusion. Interestingly, during the course of our study on the

TABLE I. Critical exponents of RTiO₃ obtained from the conventional Arrott-plot method and the MCE scaling law method and theoretical values of three models.

		α	β	γ	δ	Ref.
Arrott-plot method	Mean-field model	0	0.5	1.0	3.0	14
	3D Ising model	0.11	0.325	1.241	4.82	14
	3D Heisenberg model	-0.11	0.365	1.386	4.80	14
	DyTiO ₃	0.328(3)	1.119(2)	This paper
	HoTiO ₃	0.481(4)	1.032(2)	This paper
	ErTiO ₃	0.462(5)	0.919(2)	This paper
	TmTiO ₃	0.460(7)	1.078(2)	This paper
MCE scaling law method	YbTiO ₃	0.432(8)	1.062(3)	This paper
	YTiO ₃	-0.11 ^a	0.328(4)	1.441(5)	4.85(2)	8
	DyTiO ₃	-0.110(3) ^a	0.352(2)	1.355(3)	4.85(2)	This paper
	HoTiO ₃	-0.110(5) ^a	0.397(5)	1.476(4)	4.72(6)	This paper
	ErTiO ₃	-0.106(3) ^a	0.413(5)	1.611(6)	4.90(5)	This paper
	TmTiO ₃	-0.110(1) ^a	0.401(4)	1.427(3)	4.56(5)	This paper
	YbTiO ₃	-0.109(3) ^a	0.355(4)	1.402(3)	4.95(3)	This paper

^aThe critical exponent α is calculated from the specific heat data.

magnetocaloric effect (MCE) of these ferromagnetic RTiO₃,¹² we found that the correct critical exponents can be deduced from the MCE scaling laws.¹³

For a magnetic system with a second-order phase transition, Oesterreicher and Parker¹⁵ have proposed a universal relation:

$$|\Delta S_M^{\text{PK}}| \propto H^n \quad \text{with} \quad n = 2/3, \quad (7)$$

where ΔS_M^{PK} is the peak value of the magnetic entropy change at different external magnetic fields H . Although subsequent experimental results in some soft magnetic amorphous alloys exhibit a deviation from $n = 2/3$,¹⁶ Franco *et al.*^{13,17} recently confirmed the existence of the above universal relation and provided a new relation, i.e., the MCE scaling law:

$$n = 1 + (\beta - 1)/(\beta + \gamma), \quad (8)$$

which is in better agreement with the experimental results. In addition, the relative cooling power (RCP) obeys the scaling law:

$$\text{RCP} \propto H^{1+1/\delta}. \quad (9)$$

According to Eqs. (6)–(9), we can deduce the critical exponents β and γ by determining the values of n and δ from the field dependencies of ΔS_M^{PK} and RCP, respectively. Here, we report critical exponents for most ferromagnetic members in the RTiO₃ family by measuring the magnetocaloric effect and applying the corresponding scaling laws. Our results indicate that the ferromagnetic coupling in the RTiO₃ can be well described by the 3D Heisenberg model. The present study on RTiO₃ perovskites demonstrates that the MCE scaling laws can provide an alternative approach to investigate the critical behavior of a magnetic phase transition involving a strong paramagnetic background.

Single-crystal RTiO₃ was grown by the floating-zone method as described elsewhere.⁸ The phase purity and crystal quality were examined with powder x-ray diffraction and Laue back diffraction, respectively. DC magnetization and specific-heat measurements were performed with a Physical

Property Measurement System (PPMS-9T) from Quantum Design.

Figure 1 shows the temperature dependence of magnetization $M(T)$ for an YbTiO₃ single crystal measured upon warming up from 10 to 70 K under an external magnetic field $H = 0.01$ T after zero-field cooling (ZFC). The ferromagnetic ordering of the Ti³⁺ spins induces an abrupt increase in $M(T)$ around $T_c = 42.5$ K, leading to a large magnetic entropy change. The field-cooled cooling (FCC) and field-cooled warming (FCW) $M(T)$ curves (inset of Fig. 1) do not show any thermal hysteresis around T_c , indicating a second-order magnetic phase transition. At temperatures slightly below T_c , the magnetization decreases sharply until ~ 30 K, where the $M(T)$ curve exhibits a noticeable shoulder. In comparison with the typical ferromagnetic behavior observed in YTiO₃,⁸ these

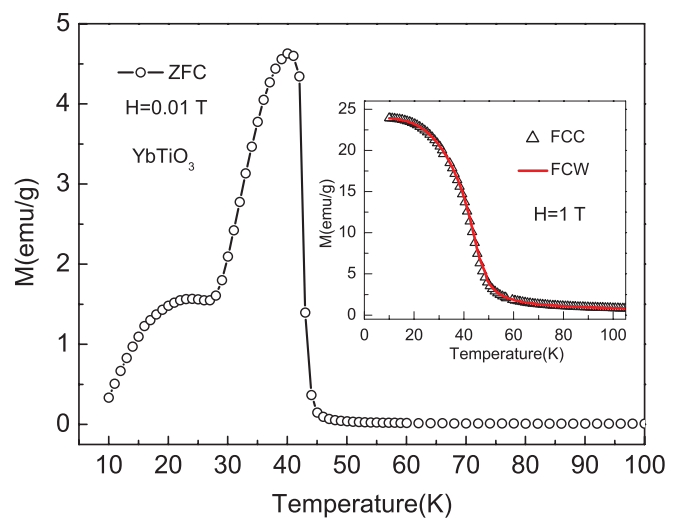


FIG. 1. (Color online) Temperature dependence of the magnetization measured at $H = 0.01$ T after zero-field cooling for an YbTiO₃ single crystal. Inset: Magnetization vs. temperature curves in the field-cooled cooling and warming cycles under a magnetic field of 1 T.

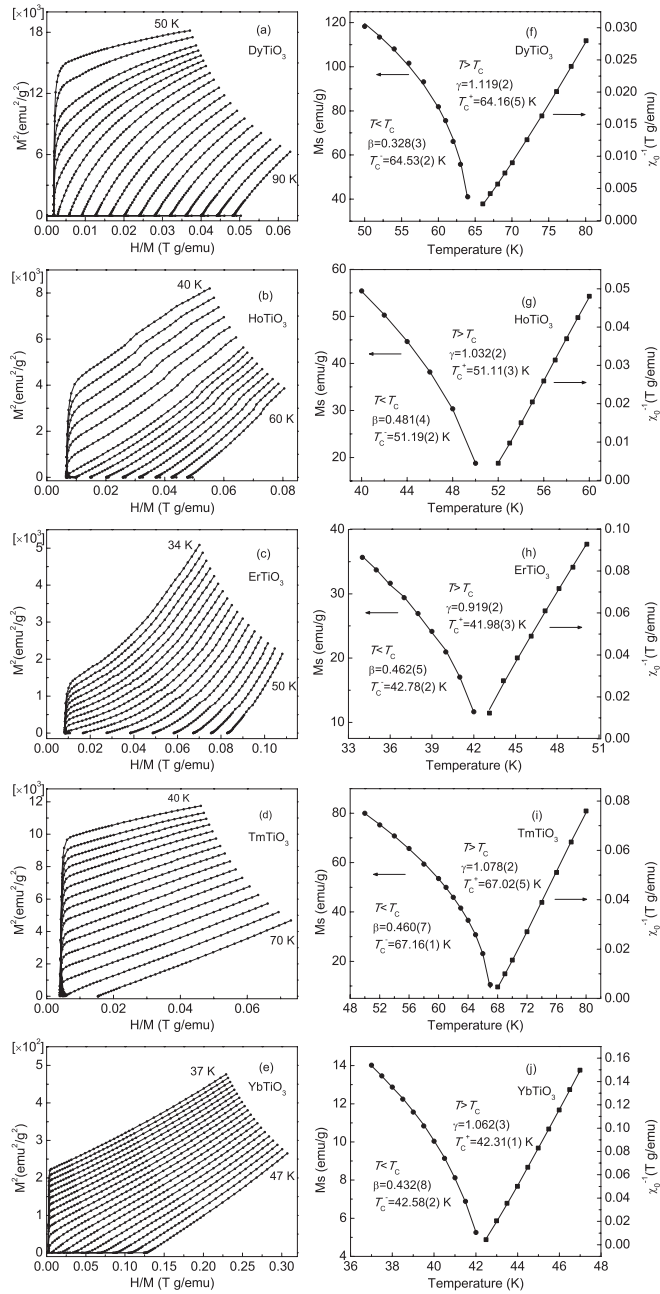


FIG. 2. (a)–(e) Arrott plots M^2 versus H/M for RTiO_3 , respectively. (f)–(j) Critical exponents, β and γ , and critical temperatures, T_c^- and T_c^+ , determined from an iteration process started from the Arrott plot for RTiO_3 , respectively.

features should arise from the large Yb^{3+} moments, and they indicate an antiparallel alignment relative to the ferromagnetic Ti^{3+} spins. As shown below by the specific-heat data, the Yb^{3+} moments do not show a long-range ordering, at least down to 20 K. The large paramagnetic contribution of the Yb^{3+} moments makes it invalid to evaluate the critical behavior near T_c using the conventional Arrott-plot method. Similar results are also found in the other RTiO_3 with magnetic R^{3+} ($\text{R} = \text{Dy}, \text{Ho}, \text{Er}, \text{Tm}$).

As shown in Fig. 2, the Arrott plots of the RTiO_3 single crystals produce nearly parallel straight lines both below and above T_c , which seem to suggest that the critical behavior

of RTiO_3 fits to the mean-field universality class.¹⁴ The critical exponents, β and γ , obtained with the conventional Arrott-plot procedure, are also close to those predicted by the mean-field model (see Table I). However, it has been well established in YTiO_3 that the critical behavior associated with the ferromagnetic ordering of the Ti^{3+} spins belongs to the 3D Heisenberg universality class.^{8,9} In addition, the nearest-neighbor exchange interactions between localized Ti^{3+} spins in these ferromagnetic RTiO_3 do not fit into the mean-field model. The large paramagnetic R^{3+} moments contribute to a linear-field dependence in the isothermal $M(H)$ curves around T_c , which significantly modifies the magnetization process and then leads to a different model of magnetic interactions based on the conventional Arrott-plot method. In the following,

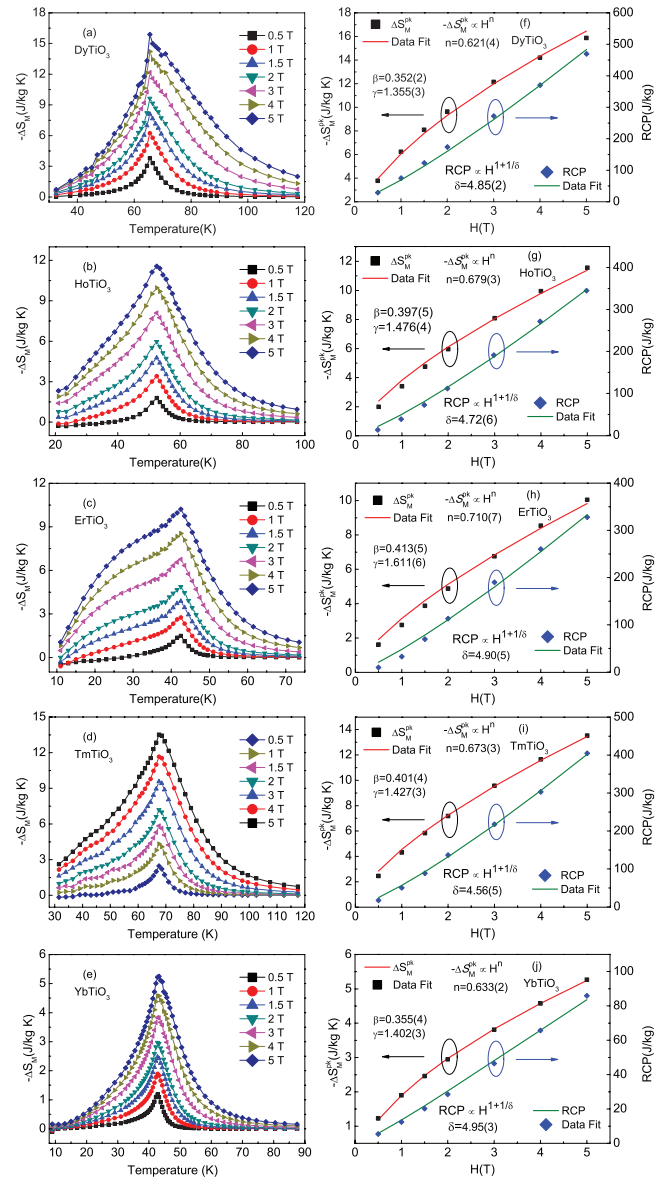


FIG. 3. (Color online) (a)–(e) Temperature dependence of the magnetic entropy changes ΔS_M under various external magnetic fields. (f)–(j) Field dependence of the maximal ΔS_M and the RCP and their fitting curves using the MCE scaling laws.

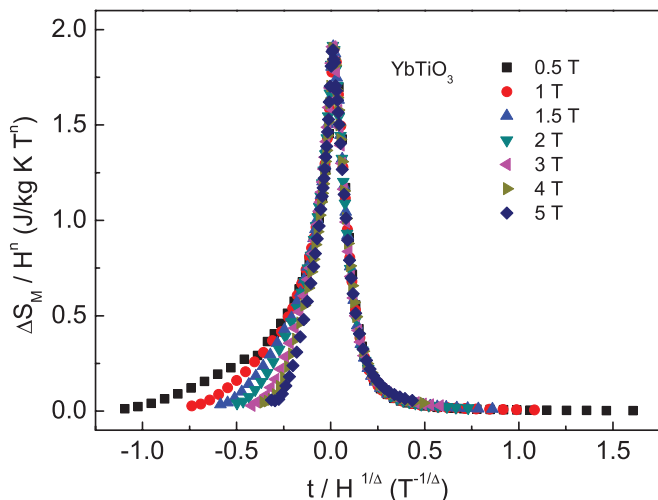


FIG. 4. (Color online) Scaling plot for YbTiO₃ below and above T_c based on the critical exponents $\beta = 0.355$, $\gamma = 1.402$, and $\delta = 4.95$ (where $n = 1 + [\beta - 1]/[\beta + \gamma]$ and $\Delta = \beta\delta$).

we show that the correct critical exponents of RTiO₃ can be deduced from the MCE scaling laws.

We have shown recently that the magnetic transitions of the ferromagnetic RTiO₃ are accompanied by a large magnetocaloric effect.¹² Here, we applied the above-mentioned MCE scaling laws to evaluate the critical behavior of RTiO₃. In order to obtain the values of n and δ , we first calculated the magnetic entropy change versus temperature under different magnetic fields by using the Maxwell relation: $\Delta S_M(T, \Delta H) = \int_0^H (\frac{\partial M}{\partial T})_H dH$. Then, the RCP (evaluated by $\text{RCP} = \Delta S_M^{\text{PK}} \times \delta T_{\text{FWHM}}$ ¹⁹) can be deduced from the ΔS_M versus T curves. The calculated $\Delta S_M(T)$ values under different magnetic fields for RTiO₃ are shown in Figs. 3(a)–3(e), while the field dependencies of ΔS_M^{PK} and RCP are plotted in

Figs. 3(f)–3(j). As shown by the solid lines in Figs. 3(f)–3(j), least-square fitting to $\Delta S_M^{\text{PK}}(H)$ and $\text{RCP}(H)$ with Eqs. (7) and (9) yields the values of n and δ , respectively. Finally, with the help of Eqs. (6) and (8), the critical exponents β and γ of RTiO₃ were determined, respectively. These values are in sharp contrast with those obtained from the Arrott-plot method shown previously. As shown in Table I, the critical exponents β and γ of RTiO₃ are close to those predicted by the 3D Heisenberg model and are in excellent agreement with those of YTiO₃.^{8,9}

The reliability of our critical-behavior analysis for RTiO₃ was further confirmed by the scaling plot of the magnetic entropy change ΔS_M ,^{17,18} which can be expressed as $\Delta S_M/a_M = H^n s(t/H^{1/\Delta})$, where $a_M = T_c^{-1} A^{\delta+1} B$ with A and B representing the critical amplitudes as in $M_s(T) = A(-t)^\beta$ and $H = B M^\delta$, respectively, $\Delta = \beta\delta$, and $s(x)$ is the scaling function. If the reduced temperature t were to be rescaled by a factor $H^{1/\Delta}$ and the magnetic entropy change ΔS_M by H^n , the experimental data should collapse onto the same curve. For instance, by using the values of $\beta = 0.355$, $\gamma = 1.402$, and $\delta = 4.95$ obtained earlier herein, we have obtained the scaling plot of Fig. 4 for our YbTiO₃ single crystal. As can be seen, except for the low temperature region at $T < T_c$, all data points indeed fall onto the same curve. Therefore, the MCE scaling method is an effective and reliable approach to investigate the critical behavior of RTiO₃ having a strong paramagnetic background near T_c .

To complete the critical-behavior analysis, we have further determined the critical exponent α from the specific-heat measurement. Figure 5 shows the specific heat $C(T)$ of RTiO₃ in the temperature range near T_c . In the critical region, $C(T)$ data can be described by a more sophisticated function:²⁰

$$C_p = B^\pm + C^\pm t + A^\pm |t|^{-\alpha} (1 + E^\pm |t|^{0.5}), \quad (10)$$

where $t = (T - T_c)/T_c$ is the reduced temperature, α is the critical exponent, and A^\pm , B^\pm , C^\pm , and E^\pm are adjustable

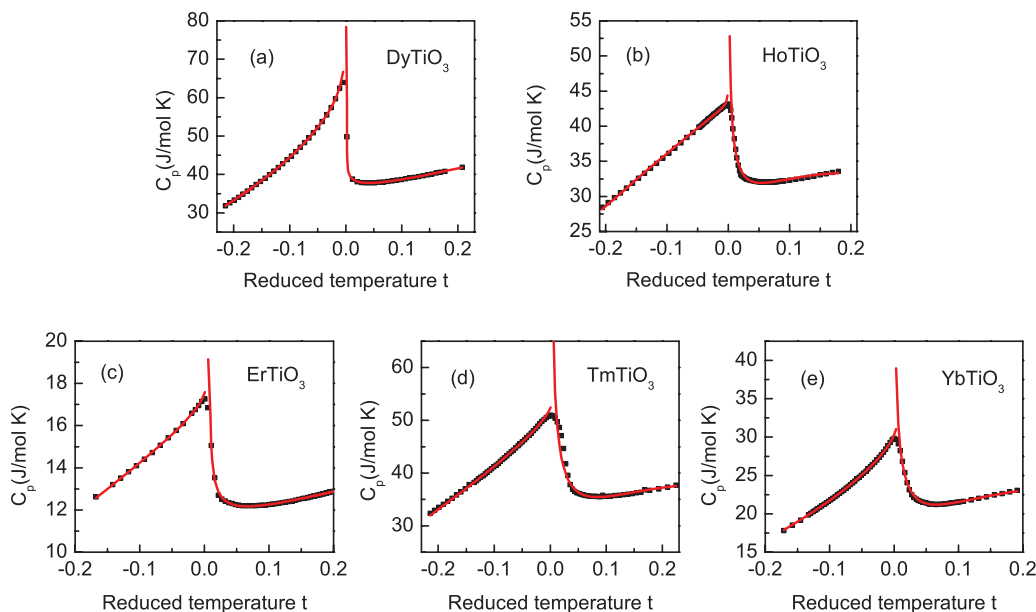


FIG. 5. (Color online) Experimental (squares) and fitted curves (continuous lines) of the specific heat as a function of the reduced temperature for the RTiO₃ in the vicinity of T_c .

TABLE II. Critical parameters, adjustable fitting parameters, fitting ranges, and quality of the fittings of the specific heat for RTiO₃. R is the deviation coefficient.

		α	T_c (K)	A (J mol ⁻¹ K ⁻¹)	B (J mol ⁻¹ K ⁻¹)	C (J mol ⁻¹ K ⁻¹)	E	$t_{\min}-t_{\max}$	R^2
DyTiO ₃	$T < T_c$	-0.110(3)	64.7 (9)	-13.5(6)	74.6(4)	9.04(9)	6.35(7)	$2.3 \times 10^{-1}-7.7 \times 10^{-3}$	0.9999
	$T > T_c$	-0.110(1)	65.1 (5)	-30.0(3)	55.4(6)	28.04(4)	-0.50(2)	$7.7 \times 10^{-3}-2.3 \times 10^{-1}$	0.9989
HoTiO ₃	$T < T_c$	-0.110(5)	50.7 (4)	-10.0(2)	48.0(9)	-97.75(3)	-2.22(9)	$2.1 \times 10^{-1}-9.8 \times 10^{-3}$	0.9993
	$T > T_c$	-0.109(2)	50.8 (6)	-200.6(3)	144.1(4)	-217.0(2)	-1.341(3)	$3.9 \times 10^{-3}-1.8 \times 10^{-1}$	0.9951
ErTiO ₃	$T < T_c$	-0.106(3)	41.7(9)	-5.0(2)	20.4(5)	-21.3(3)	0.044(1)	$1.6 \times 10^{-1}-7.2 \times 10^{-3}$	0.9998
	$T > T_c$	-0.108(1)	42.0(1)	-22.7(3)	25.6(4)	-5.90(4)	-0.88(7)	$9.6 \times 10^{-3}-2.0 \times 10^{-1}$	0.9938
TmTiO ₃	$T < T_c$	-0.110(1)	65.2(2)	-3.11(2)	54.7(4)	-49.7(3)	7.65(1)	$2.1 \times 10^{-1}-7.7 \times 10^{-3}$	0.9998
	$T > T_c$	-0.110(1)	65.2(1)	-326.7(3)	226(4)	-242.3(2)	-1.09(3)	$7.7 \times 10^{-3}-2.3 \times 10^{-1}$	0.9943
YbTiO ₃	$T < T_c$	-0.109(3)	42.2(2)	-0.738(8)	32.23(2)	-4.78(3)	50.4(3)	$1.7 \times 10^{-1}-4.8 \times 10^{-3}$	0.9998
	$T > T_c$	-0.110(3)	42.0(5)	-200(2)	135.3(1)	-168.8(2)	-1.18(8)	$7.1 \times 10^{-3}-1.9 \times 10^{-1}$	0.9937

parameters. Superscripts + and - stand for $T > T_c$ and $T < T_c$, respectively. The linear term represents the background contribution to the specific heat, whereas the last term is the anomalous contribution to the specific heat. The factor within parentheses is the correction to scaling that represents a singular contribution to the leading power as known from experiments and theory.^{21,22} As shown by the continuous line in Fig. 5, the experimental data can be described excellently with Eq. (10). The obtained critical parameters, adjustable fitting parameters (such as A, B, C, and E), the fitting ranges, and the quality of the fittings (given by the root mean square value) are listed in Table II. The fitting reduced temperature t range is about $10^{-1}-10^{-3}$ in the vicinity of T_c , while avoiding the rounding part.²³ The root mean square value R^2 is close to 1, indicating the validity of the fitting. The fitting ranges are in all cases limited by the rounding in the curves near the transition temperature; this rounding is inherent to the quality of the samples and the attribution to the measurement technique.²³ The obtained α (see Tables I and II) for RTiO₃ single crystal is in excellent agreement with the prediction of the 3D Heisenberg model,^{14,24} further supporting our analysis with the MCE scaling laws. Critical exponents α , β , and γ of RTiO₃ obtained in this study satisfy Eq. (5), $\alpha + 2\beta + \gamma = 2$, which also indicates that the critical exponents obtained by the MCE scaling law method is valid.

Finally, we briefly comment on the merit of the MCE scaling laws, which can overcome the drawback of the

conventional Arrott-plot method by avoiding the influence of the paramagnetic R^{3+} moments on the critical behavior of RTiO₃. In the critical region where the Ti^{3+} spins undergo a sharp ferromagnetic ordering, the R^{3+} moments remain paramagnetic and vary smoothly with temperature without singularity. Since the magnetic entropy change ΔS_M is proportional to the temperature derivative of the magnetization, dM/dT , the paramagnetic ‘background’ from the R^{3+} moments can be eliminated. In other words, the magnetocaloric effect at T_c mainly reflects the ferromagnetic ordering behavior of the Ti^{3+} spins. Therefore, the MCE scaling laws are valid to investigate the critical behavior of RTiO₃.

In summary, we have determined that the critical behavior in RTiO₃ single crystals belongs to the 3D Heisenberg universality class by using the MCE scaling laws, which also agree with the specific-heat measurement. This approach not only eliminates the influence of other paramagnetic contributions in the critical region, it also avoids the drawback of the iteration procedure in the conventional Arrott-plot method. Therefore, the MCE scaling laws can be applied to complex magnetic systems involving different magnetization processes in the critical region.

This paper was supported by the National Natural Science Foundation of China (Grant No. 10804024) and the National Science Foundation Materials Interdisciplinary Research Teams (Grant No. DMR-1122603) in the USA.

*Corresponding author: suiyu@hit.edu.cn

¹H. E. Stanley, *Introduction to Phase Transition and Critical Phenomena* (Oxford University Press, New York, 1971).

²M. E. Fisher, S. K. Ma, and B. G. Nickel, *Phys. Rev. Lett.* **29**, 917 (1972).

³M. Seeger, H. Kronmüller, and H. J. Blythe, *J. Magn. Magn. Mater.* **139**, 312 (1995).

⁴E. P. Wohlfarth *J. Appl. Phys.* **39**, 1061 (1968).

⁵M. Seeger, S. N. Kaul, H. Kronmüller, and R. Reisser, *Phys. Rev. B* **51**, 12585 (1995).

⁶F. Y. Yang, C. L. Chien, X. W. Li, G. Xiao, and A. Gupta, *Phys. Rev. B* **63**, 092403 (2001).

⁷J. Yang, Y. P. Lee, and Y. Li, *Phys. Rev. B* **76**, 054442 (2007), and references herein.

⁸J.-G. Cheng, Y. Sui, J.-S. Zhou, J. B. Goodenough, and W. H. Su, *Phys. Rev. Lett.* **101**, 087205 (2008).

⁹W. Knafo, C. Meingast, A. V. Boris, P. Popovich, N. N. Kovaleva, P. Yordanov, A. Maljuk, R. K. Kremer, H. v. Löhneysen, and B. Keimer, *Phys. Rev. B* **79**, 054431 (2009).

¹⁰J.-G. Cheng, J.-S. Zhou, J. B. Goodenough, Y. T. Su, and Y. Sui, *Phys. Rev. B* **83**, 212403 (2011).

¹¹A. Arrott and J. E. Noakes, *Phys. Rev. Lett.* **19**, 786 (1967).

¹²Y. T. Su, Y. Sui, J.-G. Cheng, X. J. Wang, Y. Wang, W. F. Liu, and X. Y. Liu, *J. Appl. Phys.* **110**, 083912 (2011).

- ¹³V. Franco and A. Conde, *Int. J. Refrig.* **33**, 465 (2010).
- ¹⁴H. E. Stanley, *Rev. Mod. Phys.* **71**, S358 (1999).
- ¹⁵H. Oesterreicher and F. T. Parker, *J. Appl. Phys.* **55**, 4334 (1984).
- ¹⁶Q. Y. Dong, H. W. Zhang, J. R. Sun, B. G. Shen, and V. Franco, *J. Appl. Phys.* **103**, 116101 (2008).
- ¹⁷V. Franco, A. Conde, J. M. Romero-Enrique, and J. S. Blazquez, *J. Phys.: Condens. Matter* **20**, 285207 (2008).
- ¹⁸C. M. Bonilla, J. Herrero-Albillos, F. Bartolomé, L. M. García, M. Parra-Borderías, and V. Franco, *Phys. Rev. B* **81**, 224424 (2010).
- ¹⁹B. Li, J. Du, W. J. Ren, W. J. Hu, Q. Zhang, D. Li, and Z. D. Zhang, *Appl. Phys. Lett.* **92**, 242504 (2008).
- ²⁰A. Salazar, M. Massot, A. Oleaga, A. Pawlak, and W. Schranz, *Phys. Rev. B* **75**, 224428 (2007).
- ²¹G. Ahlers, *Rev. Mod. Phys.* **52**, 489 (1980).
- ²²A. Aharony and M. E. Fisher, *Phys. Rev. B* **27**, 4394 (1983).
- ²³A. Oleaga, A. Salazar, D. Prabhakaran, J.-G. Cheng, and J.-S. Zhou, *Phys. Rev. B* **85**, 184425 (2012).
- ²⁴V. Privman, P. C. Hohenberg, and A. Aharony, in *Phase Transitions and Critical Phenomena*, edited by C. Domb and J. L. Lebowitz, Vol. 14 (Academic, New York, 1991).